Reduced coupled-mode approach to electron-ion energy relaxation

D. A. Chapman,[1,2] J. Vorberger,[3] and D. O. Gericke[2]
[1]*Plasma Physics Department, AWE plc, Aldermaston, Reading RG7 4PR, United Kingdom*
[2]*Centre for Fusion, Space and Astrophysics, Department of Physics, University of Warwick, Coventry CV4 7AL, United Kingdom*
[3]*Max-Planck-Institut für die Physik komplexer Systeme, 01187 Dresden, Germany*
(Received 4 April 2013; published 8 July 2013)

We present a reduced model for the energy transfer via coupled collective modes in two-temperature plasmas based on quantum statistical theory. The model is compared with exact numerical evaluations of the coupled-mode (CM) energy transfer rate and with alternative reduced approaches over a range of conditions in the warm dense matter (WDM) and inertial confinement fusion (ICF) regimes. Our approach shows excellent agreement with an exact treatment of the CM rate and supports the importance of the coupled-mode effect for the temperature and energy relaxation in WDM and ICF plasmas. We find that electronic damping of collective ion density fluctuations is crucial for correctly describing the mode spectrum and, thus, the energy exchange. The reduced CM approach is studied over a wide parameter space, enabling us to establish its limits of applicability.

DOI: 10.1103/PhysRevE.88.013102 PACS number(s): 52.25.Dg, 52.25.Kn

I. INTRODUCTION

Warm dense matter (WDM) and high-energy density (HED) plasmas have become the focus of intense experimental and theoretical investigations dedicated to inertial confinement fusion (ICF) [1–3], properties of extreme states of matter [4–6], and laboratory astrophysics [7,8]. The WDM regime may be loosely characterized by temperatures and densities in the ranges of $T \sim 1$–$100\,\mathrm{eV}$ and $n \sim 10^{22}$–$10^{26}\,\mathrm{cm}^{-3}$. In this regime, the ion-ion coupling parameter is often on the order of unity or above, $\Gamma_{ii} = Z_i^2 e^2 \beta_i / 4\pi\varepsilon_0 a_i \gtrsim 1$, and the electrons may be partially or even strongly degenerate, such that $D_e = n_e \Lambda_e^3 \gtrsim 1$. Here, $a_i = (3/4\pi n_i)^{1/3}$ is the mean ion separation, $\Lambda_e = \sqrt{2\pi}\hbar / p_e$ is the thermal de Broglie wavelength, and $p_e = (m_e/\beta_e)^{1/2}$ is the thermal momentum. As usual, $\beta_a^{-1} = k_B T_a$ denotes the temperature in energy units for species $a = e,i$.

Creating matter at the temperatures and densities in the WDM and HED regimes using optical lasers, free electron lasers, intense charged particle beams, or shock waves inevitably leads to strongly nonequilibrium states [4,9–12]. The energy absorbed into a particular subsystem, i.e., the electrons or the ions, is then thermalized via ultrafast processes, leading to the establishment of a two-temperature system [13]. Naturally, full thermodynamic equilibrium is eventually reached due to the exchange of energy between the different species [14–17]. This may occur by means of collisions and the interaction of collective excitations in the fully coupled multicomponent system.

Energy transfer and temperature evolution are coupled via the partial equation of state, which determines the states of matter accessible in experiments studying dielectric [18–20] and transport properties [21,22]. Quantities that critically depend on energy transfer rates are furthermore the relaxation time and the timing for equilibrium measurements [23–25]. Experimental platforms designed to investigate these properties rely heavily on large-scale radiation hydrodynamics simulations for design and optimization, and thus accurate models for the thermodynamic evolution are important.

Fully numerical approaches to modeling energy relaxation are often extremely computationally expensive, and are thus unfeasible to be run *in line*, i.e., within larger host codes such as hydrodynamics simulations. Instead, simple analytic models, e.g., those of Spitzer [26] or Brysk [27], are often implemented for simplicity. Deficiencies in the physics of these simple models can be mitigated to some extent using *ad hoc* corrections, such as modified Coulomb logarithms [28].

In this paper, we investigate the energy exchange rate between electrons and ions in a two-component plasma within a quantum statistical framework. This ensures the correct description of the particle kinetics in the dense, partially degenerate systems of interest. Following a similar approach to previous work [29–34], a reduced description of the coupled-mode (CM) theory derived by Dharma-wardana and Perrot [14], and later by Vorberger *et al.* [16,36], is developed in order to produce quick, robust, and highly accurate calculations suitable for implementation in hydrodynamics codes. We find excellent agreement with full numerical calculations for a very wide range of temperatures and densities, with a strong coupled-mode effect becoming apparent in high-density systems with $T_e \gg T_i$. In contrast, only a small effect is observed in more rarefied plasmas. As expected, for $T_e < T_i$, the rate tends to agree well with the Fermi golden rule (FGR) unless electron degeneracy becomes important, which again, results in a CM effect that acts to reduce the equilibration rate.

Our model is also compared with other reduced approaches to the energy relaxation and highlights several important issues that have led to differing interpretations concerning the role of collective modes in electron-ion equilibration. In particular, we unambiguously demonstrate the critical role played by *dynamic* electronic damping and screening in the determination of the collective-mode structure, and its subsequent impact on the relaxation rate.

To focus solely on the relaxation physics rather than the differences in models of strong coupling [37], only the weakly coupled limit, i.e., the random phase approximation (RPA), is studied here. The theoretical description is, however, kept sufficiently general for strong coupling to be included, e.g., via local field corrections (LFCs) in the response functions [38–40].

II. THEORETICAL MODEL

The energy exchange rate for a plasma of electrons and multiple species of ions, distinguishable by both their masses m_a and charges $Z_a e$, can be derived in a quantum statistical framework [14,16,41] by considering the balance equation of the total mean energy,

$$\sum_b \mathcal{Z}_{ab}(t) = \frac{\partial}{\partial t}[\langle K_a(t)\rangle + \langle V_a(t)\rangle], \tag{1}$$

where the kinetic and potential energy operators, $\hat{K}_a(t)$ and $\hat{V}_a(t)$, respectively, are evaluated using the time-dependent reduced density operators in second quantization [16]. The general result for the energy transfer rate is

$$\mathcal{Z}_{ab}(t) = -2\hbar\mathcal{V}\int\frac{d\mathbf{k}}{(2\pi)^3}\int_0^\infty\frac{d\omega}{2\pi}\omega V_{ab}(k)\,\mathrm{Im}\{iL_{ab}^<(\mathbf{k},\omega;t)\}. \tag{2}$$

$\mathcal{V}$ is the volume, $V_{ab}(k) = Z_a Z_b e^2/\varepsilon_0 k^2$ is the Coulomb interaction, and $L_{ab}^<(\mathbf{k},\omega;t)$ is the Fourier transform of the correlation function of density fluctuations between species a and b with respect to the microscopic variables. The time dependence in Eq. (2) is retained in a local approximation only, requiring that the energy exchange occurs over times much greater than the microscopic correlation times. For WDM states, one may expect relaxation times on the order of picoseconds, such that the local approximation is always well-fulfilled.

Using real-time nonequilibrium Green's functions, one obtains a self-consistent integral equation for the density response function on the Keldysh contour $\mathcal{K}$,

$$L_{ab}(12) = \Pi_{ab}(12) + \sum_{cd}\int_{\mathcal{K}} d(34)\Pi_{ac}(13)V_{cd}(34)L_{db}(42), \tag{3}$$

with $1 = \{\mathbf{r}_1, t_1, \sigma_1\}$, where σ_1 is the spin of the particle located at $\mathbf{r}_1$ at time t_1. This yields an algebraic system of linear equations in Fourier space in terms of the polarization $\Pi_{ab}(\mathbf{k},\omega)$. The latter measures the density response to the total effective potential, including the dynamic screening of the mean Coulomb field. We consider the polarization function in an approximation where cross species terms are neglected. This is justified for many WDM systems as such cross-species contributions are of second order in the interaction. Before taking into account such terms, higher-order correlations within the separate subsystems have to be considered, e.g., via LFCs. Presently, we do not explicitly account for LFCs, although they can be easily inserted (see, e.g., Refs. [14,16]).

Upon application of the Langreth-Wilkins rules [42] for functions defined on the Keldysh time contour, one finds the imaginary part of the appropriate density response of an electron-ion plasma in Fourier space [16]

$$\mathrm{Im}\{iL_{ei}^<(\mathbf{k},\omega;t)\} = 2\big[n_B^e(\omega;t) - n_B^i(\omega;t)\big] \times \frac{V_{ei}(k)\mathrm{Im}\mathcal{L}_{ee}^R(\mathbf{k},\omega;t)\mathrm{Im}\mathcal{L}_{ii}^R(\mathbf{k},\omega;t)}{\big|1 - V_{ei}^2(k)\mathcal{L}_{ee}^R(\mathbf{k},\omega;t)\mathcal{L}_{ii}^R(\mathbf{k},\omega;t)\big|^2}, \tag{4}$$

with

$$\mathcal{L}_{aa}^R(\mathbf{k},\omega;t) = \frac{\Pi_{aa}^R(\mathbf{k},\omega;t)}{1 - V_{aa}(k)\,\Pi_{aa}^R(\mathbf{k},\omega;t)}. \tag{5}$$

Here, the retarded density response and polarization functions for the species $a = e,i$ have been introduced. The time evolution of the Bose functions, $n_B^a(\omega) = [\exp(\beta_a\hbar\omega) - 1]^{-1}$, is given by their temperature dependency. Furthermore, the retarded polarization functions for weakly coupled systems can be taken in RPA, whereby they have a well-known form [41].

For an isotropic, spatially homogeneous system, all functions depend only on the wave number $k = |\mathbf{k}|$. From Eqs. (4) and (5), one thus finds the coupled-mode (CM) energy exchange rate to be

$$\mathcal{Z}_{ei}^{\mathrm{CM}}(t) = \frac{\hbar\mathcal{V}}{\pi^3}\int_0^\infty dk\,k^2\int_0^\infty d\omega\,\omega\big[n_B^i(\omega;t) - n_B^e(\omega;t)\big] \times \frac{\mathrm{Im}\varepsilon_{ee}(k,\omega;t)\,\mathrm{Im}\varepsilon_{ii}(k,\omega;t)}{|\varepsilon(k,\omega;t)|^2}. \tag{6}$$

The Bose functions determine the occupation of the collective modes whose spectral functions are given by the imaginary parts of the dielectric functions of the subsystems, $\varepsilon_{aa}(k,\omega) = 1 - V_{aa}(k)\,\Pi_{aa}^R(k,\omega)$. On the other hand, the coupling of the electron and ion modes, and the subsequent formation of the ion acoustic excitation, is determined by the full dielectric function, $\varepsilon(k,\omega) = 1 - \sum_a V_{aa}(k)\,\Pi_{aa}^R(k,\omega)$, in the denominator.

Treating the electrons and ions individually in an uncoupled electron-ion system, one obtains the Fermi golden rule (FGR) rate

$$\mathcal{Z}_{ei}^{\mathrm{FGR}}(t) = \frac{\hbar\mathcal{V}}{\pi^3}\int_0^\infty dk\,k^2\int_0^\infty d\omega\,\omega\big[n_B^i(\omega;t) - n_B^e(\omega;t)\big] \times \frac{\mathrm{Im}\varepsilon_{ee}(k,\omega;t)}{|\varepsilon_{ee}(k,\omega;t)|^2}\frac{\mathrm{Im}\varepsilon_{ii}(k,\omega;t)}{|\varepsilon_{ii}(k,\omega;t)|^2}. \tag{7}$$

Equations (6) and (7) have been obtained on the basis that all species interact via the Coulomb interaction, such that $V_{ei}(k)\,V_{ie}(k) = V_{ei}^2(k) = V_{ee}(k)\,V_{ii}(k)$, which is consistent with our approximation for the polarization function.

III. EXISTING APPROACHES TO REDUCED MODELS

Although Eqs. (6) and (7) can be evaluated numerically, this may be extremely computationally intensive for certain conditions, since a sharp plasmon peak exists when $\mathrm{Re}\varepsilon_{aa}(k,\omega) = 0$. This makes direct numerical calculations unsuitable for implementation in hydrodynamic codes.

In the case of the FGR rate (7), much of the effort expended on resolving the plasmon modes can be circumvented using a number of approximations [29–34]. Specifically, one notices that the dynamic behavior of the integrand of Eq. (7) is modulated by the spectral function of the ions, $\mathrm{Im}\varepsilon_{ii}^{-1}(k,\omega) = -\mathrm{Im}\varepsilon_{ii}(k,\omega)/|\varepsilon_{ii}(k,\omega)|^2$. This decays over significantly smaller frequency scales than that of the electrons due to the large mass difference $m_i \gg m_e$, and thus Taylor expanding the electronic term about $\omega = 0$ is justified,

i.e.,

$$\mathrm{Im}\varepsilon_{ee}^{-1}(k,\omega) \approx \omega\left[\frac{\partial}{\partial\omega}\mathrm{Im}\varepsilon_{ee}^{-1}(k,\omega)\right]_{\omega=0}. \quad (8)$$

Additionally, the Bose functions are often also expanded on the basis that the energy transferred with each electron-ion interaction is small compared to the mean thermal energy,

$$n_B^i(\omega) - n_B^e(\omega) \approx \frac{k_B}{\hbar\omega}(T_i - T_e). \quad (9)$$

The above is always appropriate for the classical ions but does not hold for highly degenerate electrons, or at moderate frequencies [35].

Applying Eqs. (8) and (9) to the FGR (7) leaves an integral over frequency that can be performed analytically using the f-sum rule for the ions,

$$\int_{-\infty}^{\infty} d\omega\,\omega\,\mathrm{Im}\varepsilon_{ii}^{-1}(k,\omega) = -\pi\omega_{pi}^2. \quad (10)$$

Here, $\omega_{pi} = (Z_i^2 e^2 n_i/\varepsilon_0 m_i)^{1/2}$ is the ion plasma frequency. If one assumes only static electronic screening, then the derivative in Eq. (8) may be simplified further by taking $\mathrm{Im}\varepsilon_{ee}^{-1}(k,\omega) \approx \mathrm{Im}\varepsilon_{ee}(k,\omega)/|\varepsilon_{ee}(k,0)|^2$. Subsequently, Eq. (7) becomes [30]

$$\mathcal{Z}_{ei}^{\mathrm{RFGR}}(t) = 2\mathcal{V}\frac{Z_i^2 e^4 n_i m_e^2 k_B}{(2\pi\hbar)^3\varepsilon_0^2 m_i}[T_i(t) - T_e(t)] \times \int_0^{\infty}\frac{dk}{k}\frac{k^4 f_e(k;t)}{\left[k^2+\kappa_e^2(t)\right]^2}, \quad (11)$$

in which $f_e(k) = [\exp(\hbar^2k^2/8p_e^2 - \eta_e) + 1]^{-1}$ is the Fermi distribution. Here, the dimensionless chemical potential η_e is defined by $\mathcal{F}_{1/2}(\eta_e) = D_e/2$ and $\mathcal{F}_j(\eta)$ is the Fermi integral of order j, as given in Ref. [41]. Furthermore, in Eq. (11) the inverse screening length κ_e is determined by

$$-V_{ee}(k)\,\Pi_{ee}^R(k,0) \overset{k\to 0}{=} \frac{\kappa_{De}^2}{k^2}\frac{\mathcal{F}_{-1/2}(\eta_e)}{D_e/2} = \frac{\kappa_e^2}{k^2}, \quad (12)$$

with $\kappa_{Da} = (Z_a^2 e^2 n_a \beta_a/\varepsilon_0)^{1/2}$ being the classical Debye wave number for species a.

The long-wavelength limit of the static dielectric screening due to electrons, $\varepsilon_{ee}(k,0) = 1 + \kappa_e^2/k^2$, is expected to be appropriate for $D_e \gtrsim 1$ due to the step function-like decay of the Fermi distribution. Accordingly, the wave numbers that contribute to the k integral in Eq. (11) will be restricted to small k values only.

In light of the simple way in which the FGR may be reduced, it is tempting to follow a similar approach to the CM energy transfer rate (6). With these approximations, one can derive a similar expression to that of Daligault and Mozyrsky [33]

$$\mathcal{Z}_{ei}^{\mathrm{DM}}(t) = 2\mathcal{V}\frac{Z_i^2 e^4 n_i m_e^2 k_B}{(2\pi\hbar)^3\varepsilon_0^2 m_i}[T_i(t) - T_e(t)] \times \int_0^{\infty}\frac{dk}{k}\frac{k^4 f_e(k;t)}{\left(k^2+\kappa_e^2(t)\right)^2}\mathcal{I}_{\omega}^{\mathrm{DM}}(k;t), \quad (13)$$

with the integral term

$$\mathcal{I}_{\omega}^{\mathrm{DM}}(k) = \int_{-\infty}^{\infty}\frac{d\omega\,\omega}{\pi\omega_{pi}^2}\mathrm{Im}\left\{\frac{V_{ii}(k)\Pi_{ii}^R(k,\omega)}{1 - V_{ii}^D(k)\Pi_{ii}^R(k,\omega)}\right\}, \quad (14)$$

where $V_{ii}^D(k) = V_{ii}(k)/\varepsilon_{ee}(k,0)$ is the statically screened Debye potential. The f-sum rule holds for all systems for which the interaction part of the Hamiltonian commutes with the density operator. This is certainly true for a Coulomb system but also for a system with a Debye-type screened interaction. Therefore, the frequency integral in Eq. (14) yields unity, and the RFGR result is recovered exactly.

This result suggests that a CM effect does not exist within the scope of these simple, although often well-fulfilled, approximations. Indeed, it was pointed out in Ref. [33] that the structure of strongly coupled ions is manifest only via the electron-ion scattering rate, which was taken to be Ziman-like and included in $\Pi_{ee}^R(k,\omega)$ using the relaxation-time approximation [43]. Accordingly, upon comparison with the rates given by Dharma-wardana and Perrot [14], the effect is to increase the energy transfer rate rather than reduce it. It is essential to understand the origin of this apparent discrepancy.

We also mention the approach of Gregori and Gericke [32]. Here, the same approximations are made and again one arrives at Eq. (13). However, in this model the form of the ion polarization function is explicitly considered with the poles at the correct RPA excitation energies. In the classical and long-wavelength limits, one has the well-known expression

$$-V_{ii}(k)\Pi_{ii}^R(k,\omega) = \frac{\kappa_{Di}^2}{k^2}\left[1 - 2x_i\mathcal{D}(x_i) + i\sqrt{\pi}x_i e^{-x_i^2}\right], \quad (15)$$

where $x_a = \omega/\sqrt{2}kv_a$, $v_a = (k_B T_a/m_a)^{1/2}$ is the thermal speed of species a, and $\mathcal{D}(x) = e^{-x^2}\int_0^x dt\, e^{t^2}$ is the Dawson function of the first kind [44].

Under a limited set of conditions, the mode structure of the ion acoustic waves occupies a frequency range where the damping is weak and the peak shape is dominated by the imaginary part of Eq. (15). It is then possible to approximate the ionic contribution to the screening by expanding about $\omega = \infty$ to obtain $-V_{ii}(k)\,\Pi_{ii}^R(k) \approx -\kappa_{Di}^2/2k^2x_i^2$. The resulting frequency integral can be performed analytically and yields a k-dependent correction factor to the integrand of the RFGR Eq. (11),

$$\mathcal{Z}_{ei}^{\mathrm{GG}}(t) = 2\mathcal{V}\frac{Z_i^2 e^4 n_i m_e^2 k_B}{(2\pi\hbar)^3\varepsilon_0^2 m_i}[T_i(t) - T_e(t)] \times \int_0^{\infty}\frac{dk}{k}\frac{k^4 f_e(k;t)}{\left(k^2+\kappa_e^2(t)\right)^2}\mathcal{I}_{\omega}^{\mathrm{GG}}\left(\frac{c_s(k;t)}{\sqrt{2}v_i(t)}\right), \quad (16)$$

with the analytic integral term

$$\mathcal{I}_{\omega}^{\mathrm{GG}}(x) = |1 - 2x^2(x^2-2) + 2x^3(2x^2-5)\mathcal{D}(x) + i\sqrt{\pi}x^3(2x^2-5)e^{-x^2}|. \quad (17)$$

Here, $c_S(k)$ is a generalized sound speed, which may be left as a free fitting parameter.

IV. NEW APPROACH TO A REDUCED COUPLED-MODES MODEL

The nominally well-fulfilled approximations (8) and (9) yield reduced models for the energy exchange rate, which can be rapidly and robustly evaluated, and hence run in line in larger host codes. For the FGR, reasonably accurate results are obtained except at low electron temperatures, where the

expansion of the Bose function (9) is known to break down. On the other hand, applying the same approach to the CM effect yields results in stark contradiction with numerical evaluations of the full CM (6). Indeed, the resulting relaxation rates are then similar to, or even *faster*, than the FGR.

The origin of this apparent contradiction is, in fact, remarkably straightforward to explain. In the derivation of the reduced models discussed previously, the electronic contribution to the two-component dielectric function is treated in the static limit. As such, the functions $\varepsilon(k,\omega)$ and $\varepsilon_{ii}(k,\omega)$ differ only in the real part. Therefore, the positions of the collective ion modes, roughly given by $\mathrm{Re}\varepsilon(k,\omega)=0$, are correctly changed from quasiparticle character to an acoustic dispersion relation. However, the damping of the modes remains determined by the ions only due to the neglect of the electronic contribution. The immediate consequence of this is the existence of a very weakly damped collective ion mode with a large weight and a peak structure that grows exponentially sharper as the resonance is shifted to higher frequencies.

Of course, the range of the frequency integration is dominated by the decay of the ionic term $\mathrm{Im}\Pi^R_{ii}(k,\omega)$ and, thus, the electrons may always be treated in the low-frequency limit. However, this alone does not justify neglecting the imaginary component of $\varepsilon_{ee}(k,\omega)$. For small frequencies, the imaginary part scales roughly linearly with ω and becomes *more* important to the determination of the total mode structure as the peak is shifted to higher frequencies. Recognizing this fact, we pursue a reduced model based on the same set of approximations as before but explicitly retain the imaginary contribution to the screening in lowest order. The lowest order, nonvanishing terms of the Taylor expansion of the electron polarization are

$$-V_{ee}(k)\Pi^R_{ee}(k,\omega)\approx\frac{\kappa^2_{De}}{k^2}\left[\frac{\mathcal{F}_{-1/2}(\eta_e)}{D_e/2}+i\sqrt{\pi}x_e\frac{f_e(k)}{D_e/2}\right]. \quad (18)$$

Here, the real part has been taken in the long wavelength limit, as per Eq. (12), whereas the imaginary part is correct for arbitrary k.

By writing $\kappa^2_{De}=\mathcal{R}_1\kappa^2_{Di}$, with $\mathcal{R}_1=T_in_e/Z_i^2n_iT_e$, to map the electron Debye wave number onto that of the ions and, similarly, $x_e=\mathcal{R}_2x_i$, with $\mathcal{R}_2=(T_im_e/T_em_i)^{1/2}$, to appropriately scale the dimensionless frequency, we find the following expression for the total dielectric function

$$\varepsilon^{\mathrm{RCM}}(k,\omega)\approx 1+\frac{\kappa^2_{Di}}{k^2}\left[1-2x_i\mathcal{D}(x_i)+\mathcal{R}_1\frac{\mathcal{F}_{-1/2}(\eta_e)}{D_e/2}\right] +i\sqrt{\pi}x_i\frac{\kappa^2_{Di}}{k^2}\left[e^{-x_i^2}+\mathcal{R}_1\mathcal{R}_2\frac{f_e(k)}{D_e/2}\right]. \quad (19)$$

Substituting Eqs. (9) and (19) into Eq. (6), we arrive at the reduced coupled-modes (RCM) relaxation rate

$$\mathcal{Z}^{\mathrm{RCM}}_{ei}(t)=2\mathcal{V}\frac{Z_i^2e^4n_im_e^2k_B}{(2\pi\hbar)^3\varepsilon_0^2m_i}[T_i(t)-T_e(t)] \times\int_0^\infty dk\, f_e(k;t)\,\mathcal{I}^{\mathrm{RCM}}_\omega(k;t)\,, \quad (20)$$

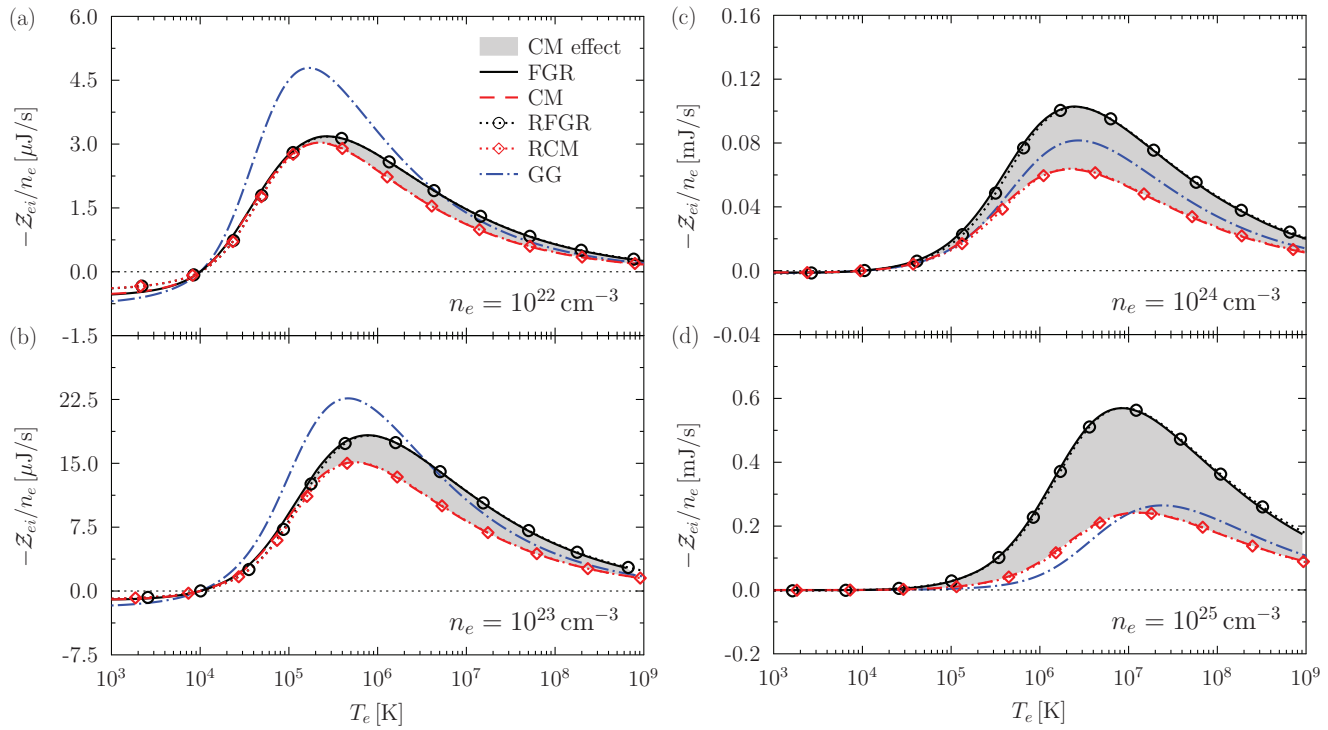

FIG. 1. (Color online) Full numerical calculations of the FGR (solid black curve) and CM (dashed red curve) energy-transfer rates compared to the reduced FGR (dotted black curve with circles) and reduced CM (dotted red curve with diamonds) approximations, with $Z_i=1$ and $T_i=10^4$ K; (a) $n_e=10^{22}\,\mathrm{cm}^{-3}$, (b) $n_e=10^{23}\,\mathrm{cm}^{-3}$, (c) $n_e=10^{24}\,\mathrm{cm}^{-3}$, (d) $n_e=10^{25}\,\mathrm{cm}^{-3}$. The model of Gregori and Gericke [32] (labeled as GG) is also shown for comparison (dash-dotted blue curve), in which the sound speed is taken to be $c_S(k)=[Z_ik_BT_e/m_i(1+k^2/\kappa_e^2)]^{1/2}$. The changes to the rates due to the coupled-mode effect are highlighted by the gray shaded region in each panel.

with

$$\mathcal{I}_{\omega}^{\mathrm{RCM}}(k) = \frac{4}{\sqrt{\pi}} \int_0^{\infty} dx \, \frac{x^2 e^{-x^2}}{\left|\varepsilon^{\mathrm{RCM}}(k,x)\right|^2}, \tag{21}$$

where $x \equiv x_i$. Note that by setting $\mathrm{Im}\varepsilon_{ee}(k,\omega) = 0$, one recovers the RFGR Eq. (11), as expected.

Clearly, Eq. (21) is not amenable to a simple analytic solution and must be solved numerically. The focus of this work now shifts to making the required numerics as efficient and optimized as possible in order to minimize computational effort. Although our model still requires a double integration, the forms of the polarization functions Eqs. (15) and (18) allow for large savings in computational intensity, making our model feasible to run in line. In particular, the Dawson function and Fermi-Dirac integrals of half-integer order can be inexpensively evaluated to high accuracy using the schemes described by Roy [45] and Lether [46].

Although a sharp peak in the integrand in Eq. (21) still occurs for some conditions, the damping afforded by the electrons guarantees that its amplitude increases more slowly than its width, and hence its contribution to the integral decreases [36]. Moreover, the position of the peak can be estimated *a priori* from the dispersion relation given by the root of the real part of Eq. (19), which is valid for small to moderate wave numbers. A small range on either side of the root of this function can then be finely resolved to adequately capture the peak structure, whereas the remainder of the integrand shows a smooth behavior.

For large wave numbers, the dispersion relation ceases to accurately predict the peak position, potentially focusing the finely resolved grid away from the detailed structure. Fortunately, both components of the damping also increase with k and grow fast enough to smooth the peak as it is shifted away from its predicted position. In fact, when the resonance occurs at sufficiently high frequency, the peak is suppressed altogether, since the integrand is modulated by the exponential decay of $\mathrm{Im}\Pi_{ii}^{R}(k,\omega)$. Moreover, if no root exists in the dispersion relation, i.e., $\mathrm{Re}\varepsilon(k,\omega) > 0$ for all ω, a sharply peaked structure does not occur at all. In both of these cases, the entire integrand is smooth and can be evaluated quickly and accurately on a coarse grid.

Figure 1 shows our RCM model, Eqs. (19)–(21) and the RFGR (11) compared to fully numerical solutions of Eqs. (6) and (7) for a fully ionized hydrogen plasma ($Z_i = 1$) at various densities. The ion temperature is fixed at $T_i = 10^4$ K in all cases. For each density, we observe generally good agreement between the RCM and CM calculations for $T_e > T_i$, with a pronounced coupled-mode effect (shaded gray regions) visible for higher densities. For example, for $T_e \geqslant 10^5$ K, the maximum relative error is $<10\%$ for all densities considered. As $T_e \to T_i$, the agreement gets worse, with the higher density results diverging faster. Calculations for higher ion temperatures also show similar agreement and the same trends in the absolute error as a function of T_e/T_i.

Figure 2 shows the low-temperature behavior around thermal equilibrium for the same range of densities. Here, the absolute difference ranges between $<20\%$ and $>570\%$ for the highest density. This trend of poor agreement at high degeneracy is consistent with the breakdown of the approximation (9) for the Bose functions. Indeed, a similar trend can be seen comparing full and reduced approaches to the FGR [35].

As expected, the disagreement is reduced for a range of temperatures about equilibrium for higher ion temperatures,

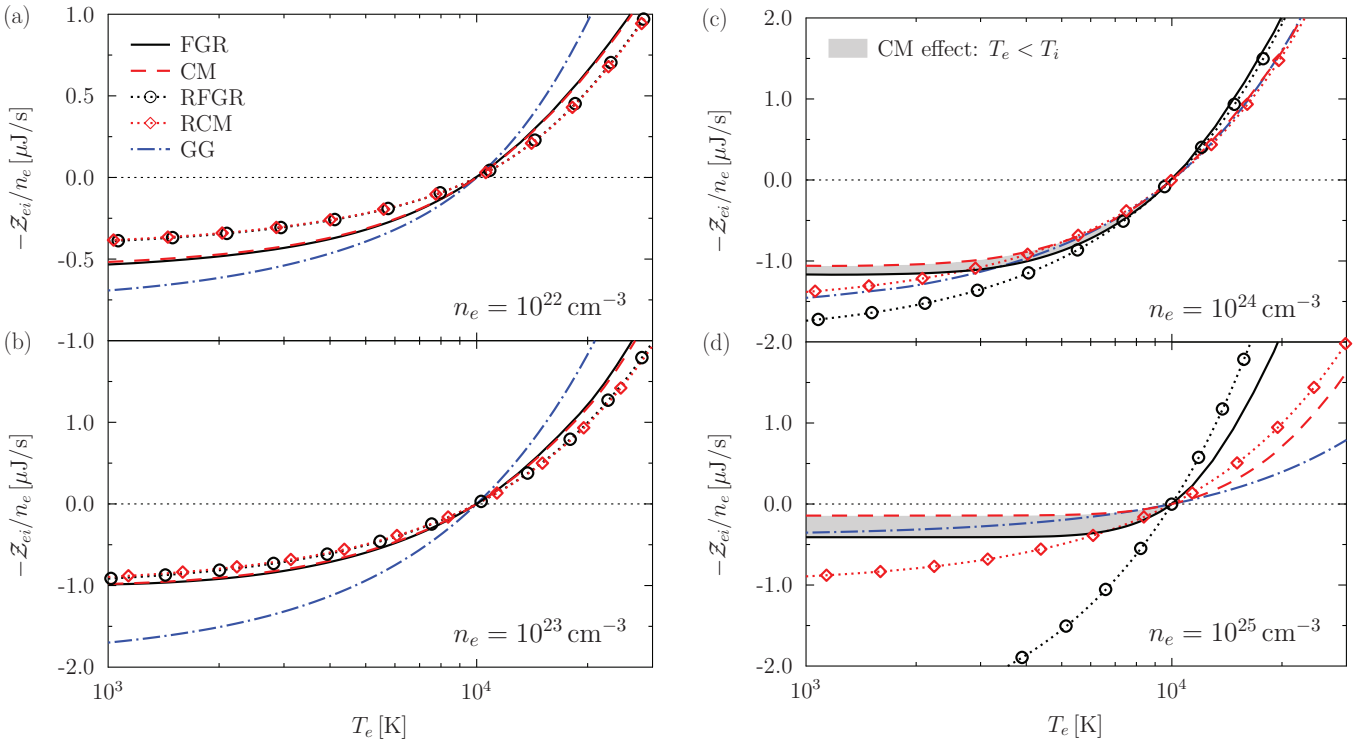

FIG. 2. (Color online) Low-temperature behavior of the energy exchange rates. All parameters are as described in the legend of Fig. 1.

e.g., $T_i = 10^5$ K, since the temperature ratio tends to unity for higher electron temperatures for a given density. Contrary to this trend is the observation that the low-temperature error seems to have a minimum for $n_e = 10^{23}\,\mathrm{cm}^{-3}$, with the agreement worsening again for decreasing density. It is also interesting to note that a CM effect is seen for $T_e < T_i$ for highly degenerate systems, as shown by the gray shaded regions in Figs. 2(c) and 2(d). This is easily explained, since for $D_e \gg 1$, we have $k_B T_e < E_F$, and thus a CM effect may exist provided that $E_F > k_B T_i$.

In contrast to the results of the new RCM model, the reduced model from Ref. [32] (labeled GG in Figs. 1 and 2) does not generally give similarly accurate results, although better agreement is seen for the highest densities considered. Specifically, the GG model is reasonable for conditions where the ion plasmon peak is pushed to higher frequencies, e.g., for high density, where the expansion of Eq. (15) is appropriate. For lower densities, the trend for the GG model is to overestimate the rate, even giving relaxation rates in excess of the FGR. Such behavior is a clear indication of the unsuitability of the model, since the FGR is the maximum rate for energy transfer via collective modes.

V. IMPROVEMENT OF THE NEW MODEL

We now attempt to improve the general accuracy of our model by considering three simple extensions: (i) including further terms in the Taylor series (18), (ii) considering the full k-dependence of the electronic contribution to the screening, and (iii) the true structure of the Bose functions.

The next nonvanishing terms in the Taylor expansion of $\Pi^R_{ee}(k,\omega)$ can be found to give the simple corrections

$$C_1(k,\omega) = 1 - 2x_e^2 \frac{\mathcal{F}_{-3/2}(\eta_e)}{\mathcal{F}_{-1/2}(\eta_e)}, \tag{22}$$

$$C_2(k,\omega) = 1 - x_e^2(1 - f_e(k))\left[1 - \frac{2q_e^2}{3}(1 - 2f_e(k))\right], \tag{23}$$

where $q_e = \hbar k/\sqrt{8}p_e$. Equations (22) and (23) now multiply the appropriate components of Eq. (18), i.e.,

$$-V_{ee}(k)\,\Pi^R_{ee}(k,\omega) \approx \frac{\kappa_{De}^2}{k^2}\left[\frac{\mathcal{F}_{-1/2}(\eta_e)}{D_e/2}C_1(k,\omega) + i\sqrt{\pi}x_e\frac{f_e(k)}{D_e/2}C_2(k,\omega)\right]. \tag{24}$$

As before, the real part is taken in the long wavelength limit, whereas the full k-dependence is retained in the imaginary part.

It can readily be shown that one recovers from Eqs. (22) and (23) the correct terms for the expansion of the polarization function in the nondegenerate and classical limits, respectively. Due to their simple form, it is no additional effort to incorporate these corrections, although we find no discernible effect for any of the conditions considered in this work. This is not surprising given the shape of $\Pi^R_{ee}(k,\omega)$ for very small frequencies.

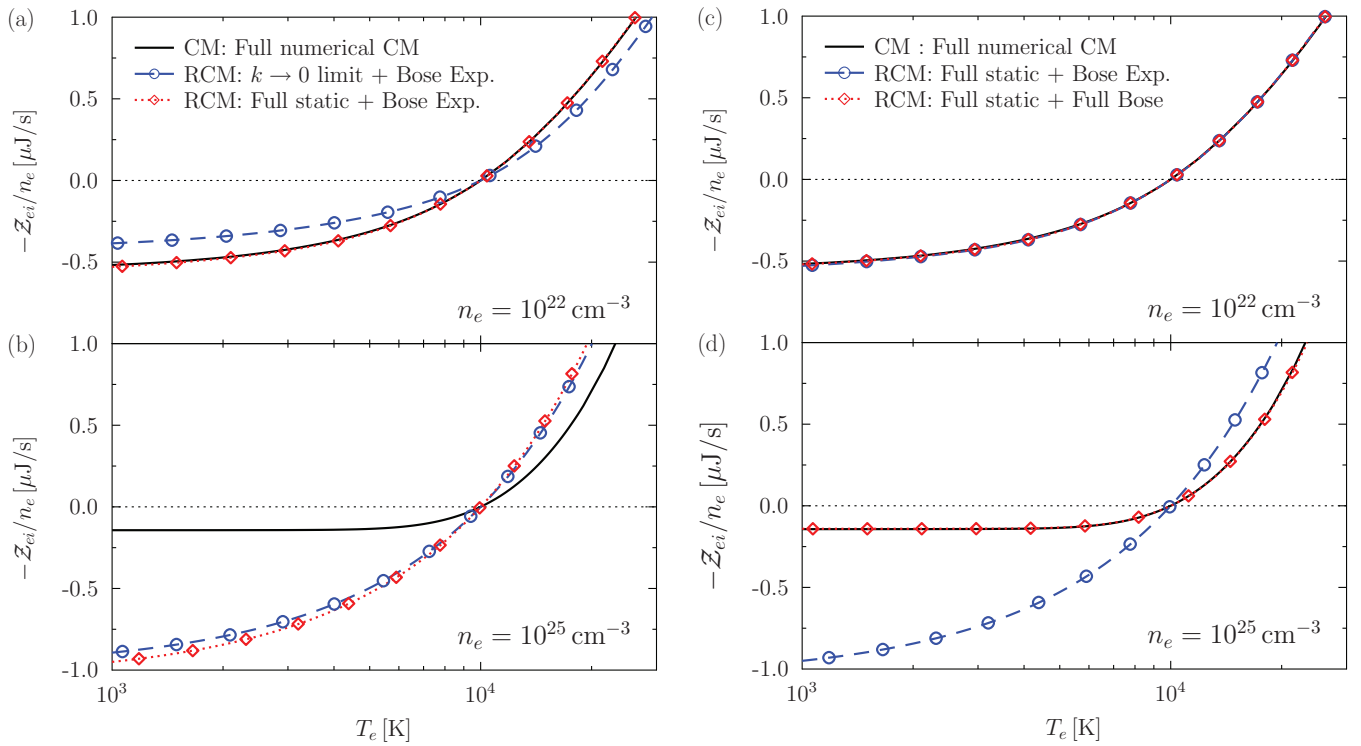

FIG. 3. (Color online) Effect of improvements to the RCM model compared to full numerical CM calculations (solid black curve) around thermal equilibrium for $T_i = 10^4$ K, in both diffuse ($n_e = 10^{22}\,\mathrm{cm}^{-3}$) and dense ($n_e = 10^{25}\,\mathrm{cm}^{-3}$) hydrogen plasmas. Panels (a) and (b) consider the usual expansion of the Bose functions given by Eq. (9) and compare the cases with long wavelength, i.e., $k \to 0$, screening only (blue dashed curves with circles), and the full static screening (red dotted curves with diamonds), as implemented in Ref. [47]. Conversely, panels (c) and (d) consider full static screening and compare the cases with the expanded structure (blue dashed curves with circles) and full structure (red dotted curves with diamonds) of the Bose functions.

Since the expansion of the Bose functions Eq. (9) is appropriate for low degeneracy, and the higher-order corrections (22) and (23) are negligible, it is reasonable to conclude that the long wavelength approximation to the electronic screening is responsible for the poor accuracy of our model for $T_e < T_i$ in the low-density case. The overestimation of the rates in this regime occurs because $f_e(k)$ is roughly Gaussian for $D_e \ll 1$ and, thus, has a long tail that does not lead to the same suppression of the integrand for large wave numbers.

Numerical evaluation of the static RPA dielectric function for arbitrary wave numbers shows that electronic screening decays significantly faster than the Debye-like inverse square scaling obtained within the long wavelength limit. In order to account for the deviation between the $k \to 0$ limit and full k-dependence of the static screening at large wave numbers, we use the parametrization presented in Ref. [47], which does not noticeably increase the computational effort of the RCM model. Conversely, for higher degeneracies, the full k-dependence of the screening is not important, as the Fermi distribution tends to a step function [see Fig. 3(a)].

On the other hand, Fig. 3(b) shows that including the full form of the Bose functions has no effect for low-density plasmas, where the low-frequency expansion holds. However, the expansion of the Bose functions account for nearly all the difference to the full numerical results at higher degeneracies.

With the simple improvements to the basic model, given by Eqs. (19)–(21), we find that the maximum absolute error between the RCM and CM calculations is now <7% for all temperatures and densities considered. In fact, this upper limit mainly arises due to the imperfection of the interpolation formula used for the full k-dependence of the static screening, and generally we see mean absolute errors of 0.5–3% (see Fig. 4). On the basis of this agreement, we unambiguously demonstrate the importance of several key issues: First and foremost, the electronic contribution to the damping is crucial in determining the proper mode structure, in particular, the damping of the ion wave onto an acoustic dispersion relation. Second, non-Debye screening cannot generally be ignored, especially in low-density plasmas. Finally, the correct structures of the Bose functions are essential for describing the rates at low temperatures in degenerate plasmas. We also find that the improved model now runs over 300 times faster than full numerical calculations, allowing it to be run inline within a host hydrodynamics code.

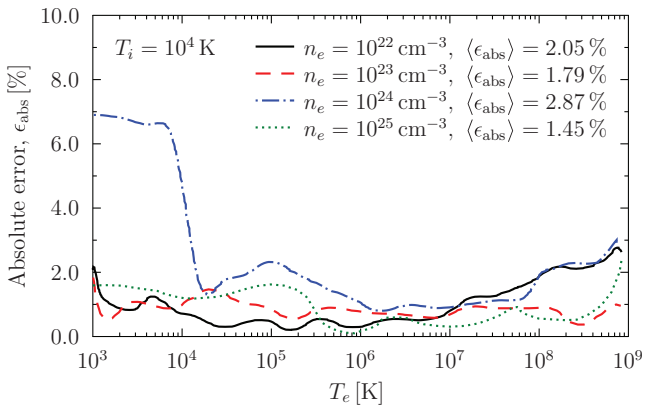

FIG. 4. (Color online) Absolute percentage error between the *full* CM calculations and reduced model described in this work, i.e., $\epsilon_{\rm abs} = 100 \times |(\mathcal{Z}_{ei}^{\rm RCM} - \mathcal{Z}_{ei}^{\rm CM})/\mathcal{Z}_{ei}^{\rm CM}|$, as a function of electron temperature. The full k-dependence and proper structure of the Bose functions are both accounted for in the RCM results presented here.

VI. SUMMARY

We have investigated the energy transfer rate in two-temperature plasmas using a quantum statistical framework, allowing a full and rigorous analysis of the role played by coupled-mode effects in WDM and dense plasmas. A number of approximations aimed at reducing the numerical effort required to evaluate the rates were presented, along with several models for both the FGR and CM descriptions. In the case of the FGR, the well-known reduced result [29,30] was recovered.

Application of the same set of approximations to the CM description revealed that no difference to the RFGR rates should be present, as suggested in Ref. [33]. This fact is in contradiction with detailed fully numerical calculations of the CM rates. We resolved this discrepancy by considering a more consistent model of the electronic contribution to the screening that included all lowest order nonvanishing terms in the Taylor expansion of $\Pi_{ee}^R(k,\omega)$. We constructed a new reduced model for the CM effect by simply keeping the imaginary part of the electronic contribution to $\varepsilon(k,\omega)$.

The resulting ω-integration could no longer be treated analytically. Thus, we focused on minimizing the computational cost of our calculations. In particular, we used simple analytic parametrizations for all relevant quantities that are usually evaluated numerically. Our results showed generally good agreement with the full CM calculations of the relaxation rate for $T_e \gg T_i$, with better than 10% accuracy achieved over the full range of densities considered. For $T_e \lesssim T_i$, some significant deviations were observed, especially for high degeneracies. We concluded that these errors arise from the Bose function expansion for conditions where the mode structure is shifted to higher frequencies. This finding is supported by the analysis presented in Ref. [35].

Finally, we abandoned most approximations for the reduced models in order to account for previously neglected physics. We considered the next-lowest-order, nonvanishing terms in the low-frequency expansion of the electronic polarization function, which showed no discernible effect. We then included the correct k-dependence in the static electronic screening by means of a simple parametrization, valid for arbitrary degeneracy, and also the true form of the Bose functions. None of these extensions noticeably increased the computational intensity of our model. We found that for low degeneracies the screening was the most important effect, while for higher degeneracies the expansion of the Bose functions constituted the most significant difference to the full CM calculations. The extended model gave results with an overall mean absolute error of ~2% over the full range of temperatures and densities considered.

With the analysis presented, we have elucidated the critical role played by the electrons to not only change the dispersion relation of the ion density waves from plasmon-like to

acoustic but *also* to crucially change the damping of the collective ion mode, which directly leads to the CM effect. Moreover, we have shown that electron damping need only be considered to first order in frequency to reproduce the full rates in two-component plasmas. Finally, our model has been made efficient enough to be incorporated in large-scale hydrodynamics simulations. This will enable estimates of the importance of the CM effect for simulations of systems such as imploding ICF capsules.

ACKNOWLEDGMENT

The authors thank the UK's Engineering and Physical Sciences Research Council for financial support of this work.

[1] S. H. Glenzer *et al.*, Science **327**, 1228 (2010).
[2] A. J. Mackinnon *et al.*, Phys. Rev. Lett. **108**, 215005 (2012).
[3] H. F. Robey *et al.*, Phys. Rev. Lett. **108**, 215004 (2012).
[4] D. Riley, N.C. Woolsey, D. McSherry, I. Weaver, A. Djaoui, and E. Nardi, Phys. Rev. Lett. **84**, 1704 (2000).
[5] A. Ravasio *et al.*, Phys. Rev. Lett. **99**, 135006 (2007).
[6] E. Garcia Saiz *et al.*, Nat. Phys. **4**, 940 (2008).
[7] J. Daligault and S. Gupta, Astrophys. J. **703**, 994 (2009).
[8] N. A. Tahir *et al.*, Astrophys. Space Sci. **336**, 61 (2011).
[9] A. Ng, P. Celliers, G. Xu, and A. Forsman, Phys. Rev. E **52**, 4299 (1995).
[10] R. R. Fäustlin *et al.*, Phys. Rev. Lett. **104**, 125002 (2010).
[11] D. A. Chapman and D. O. Gericke, Phys. Rev. Lett **107**, 165004 (2011).
[12] T. G. White *et al.*, Scientific Reports **2**, 889 (2012).
[13] B. Ziaja, A. R. B. de Castro, E. Weckert, and T. Möller, Euro. Phys. J. D **40**, 365 (2006).
[14] M. W. C. Dharma-wardana and F. Perrot, Phys. Rev. E **58**, 3705 (1998).
[15] J. N. Glosli, F. R. Graziani, R. M. More, M. S. Murillo, F. H. Streitz, M. P. Surh, L. X. Benedict, S. Hau-Riege, A. B. Langdon, and R. A. London, Phys. Rev. E **78**, 025401(R) (2008).
[16] J. Vorberger, D. O. Gericke, Th. Bornath, and M. Schlanges, Phys. Rev. E **81**, 046404 (2010).
[17] L. X. Benedict *et al.*, Phys. Rev. E **86**, 046406 (2012).
[18] S. H. Glenzer *et al.*, Phys. Rev. Lett. **98**, 065002 (2007).
[19] H. J. Lee *et al.*, Phys. Rev. Lett. **102**, 115001 (2009).
[20] P. Neumayer *et al.*, Phys. Rev. Lett. **105**, 075003 (2010).
[21] J. F. Benage, Phys. Plasmas **7**, 2040 (2000).
[22] J. Haun, H.-J. Kunze, S. Kosse, M. Schlanges, and R. Redmer, Phys. Rev. E **65**, 046407 (2002).
[23] S. P. Regan *et al.*, Phys. Rev. Lett. **109**, 265003 (2012).
[24] S. Kraus *et al.*, High Energy Density Physics **8**, 46 (2012).
[25] T. Ma *et al.*, Phys. Rev. Lett. **110**, 065001 (2013).
[26] L. Spitzer, Jr., *Physics of Fully Ionized Gases* (Wiley, New York, 1956).
[27] H. Brysk, Plasma Phys. **16**, 927 (1974).
[28] D. O. Gericke, M. S. Murillo, and M. Schlanges, Phys. Rev. E **65**, 036418 (2002).
[29] G. Hazak, Z. Zinamon, Y. Rosenfeld, and M. W. C. Dharma-wardana, Phys. Rev. E **64**, 066411 (2001).
[30] D. O. Gericke, J. Phys.: Conf. Series **11**, 111 (2005).
[31] J. Daligault and D. Mozyrsky, Phys. Rev. E **75**, 026402 (2007).
[32] G. Gregori and D. O. Gericke, Euro. Phys. Lett. **83**, 15002 (2008).
[33] J. Daligault and D. Mozyrsky, High Energy Density Physics **4**, 58 (2008).
[34] J. Daligault and G. Dimonte, Phys. Rev. E **79**, 056403 (2009).
[35] J. Vorberger and D. O. Gericke (unpublished).
[36] J. Vorberger and D. O. Gericke, Phys. Plasmas **16**, 082702 (2009).
[37] S. Ichimaru, Rev. Mod. Phys. **54**, 1017 (1982).
[38] S. Ichimaru, *Statistical Plasma Physics*, Vol. II (Addison-Wesley, Reading, MA, 1994).
[39] J. Vorberger, Z. Donko, I. M. Tkachenko, and D. O. Gericke, Phys. Rev. Lett. **109**, 225001 (2012).
[40] C. Fortmann, A. Wierling, and G. Röpke, Phys. Rev. E **81**, 026405 (2010).
[41] D. Kremp, M. Schlanges, and W.-D. Kraeft, *Quantum Statistics of Nonideal Plasmas* (Springer, Berlin, 2005).
[42] D. C. Langreth and J. W. Wilkins, Phys. Rev. B **6**, 3189 (1972).
[43] N. D. Mermin, Phys. Rev. B **1**, 2362 (1970).
[44] M. Abramowitz and I. A. Stegun, *Handbook of Mathematical Functions* (Dover, New York, 1972).
[45] D. Roy, Comput. Phys. Comm. **180**, 1315 (2009).
[46] F. G. Lether, J. Sci. Comput. **15**, 479 (2000).
[47] R. G. Dandrea, N. W. Ashcroft, and A. E. Carlsson, Phys. Rev. B **34**, 2097 (1986).